

# Temperature- and Component-Dependent Degradation of Perovskite Photovoltaic Materials under Concentrated Sunlight

Ravi K. Misra,<sup>†</sup> Sigalit Aharon,<sup>‡</sup> Baili Li,<sup>†</sup> Dmitri Mogilyansky,<sup>§</sup> Iris Visoly-Fisher,<sup>†,§</sup> Lioz Etgar,<sup>‡</sup> and Eugene A. Katz<sup>\*,†,§</sup>

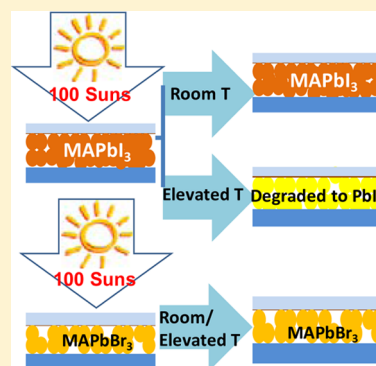
<sup>†</sup>Department of Solar Energy and Environmental Physics, The Jacob Blaustein Institutes for Desert Research (BIDR), Ben-Gurion University of the Negev, Sede Boker Campus, Midereshet Ben-Gurion 84990, Israel

<sup>‡</sup>Casali Center for Applied Chemistry, The Institute of Chemistry, The Hebrew University of Jerusalem, Edmond J. Safra Campus, Givat Ram, Jerusalem 91904, Israel

<sup>§</sup>Ilse Katz Institute for Nanoscale Science & Technology, Ben Gurion University of the Negev, Beer Sheva 84105, Israel

## S Supporting Information

**ABSTRACT:** We report on accelerated degradation testing of MAPbX<sub>3</sub> films (X = I or Br) by exposure to concentrated sunlight of 100 suns and show that the evolution of light absorption and the corresponding structural modifications are dependent on the type of halide ion and the exposure temperature. One hour of such exposure provides a photon dose equivalent to that of one sun exposure for 100 hours. The degradation in absorption of MAPbI<sub>3</sub> films after exposure to 100 suns for 60 min at elevated sample temperature (~45–55 °C), due to decomposition of the hybrid perovskite material, is documented. No degradation was observed after exposure to the same sunlight concentration but at a lower sample temperature (~25 °C). No photobleaching or decomposition of MAPbBr<sub>3</sub> films was observed after exposure to similar stress conditions (light intensity, dose, and temperatures). Our results indicate that the degradation is highly dependent on the hybrid perovskite composition and can be light- and thermally enhanced.



Hybrid inorganic–organic halide perovskites emerged as a visible-light sensitizer for photovoltaics (PV) in 2009<sup>1</sup> and proved to function as an absorber and charge transporter in both solid-state mesoporous solar cell and standard planar thin-film PV architectures.<sup>2</sup> Power conversion efficiency (PCE) of perovskite-based solar cells has recently surpassed 20%.<sup>3,4</sup> Simple preparation, low cost, and good optical and electronic properties are some of the advantages of these inorganic–organic hybrid materials.<sup>5–7</sup> Their general chemical formula is AMX<sub>3</sub> (where A = organic cation, M = divalent metal such as Pb, Sn, and X = halide ions),<sup>5–7</sup> and the crystal structure is based on octahedral metal halide in the form of [MX<sub>6</sub>]<sup>4–</sup> surrounded by eight organic cations in a tetragonal or cubic arrangement (Figure 1). Methylammonium lead halide perovskites (MAPbX<sub>3</sub>) is the most promising class of perovskite materials for PV applications with the additional advantage of tuning their properties by varying the type of halide ions.<sup>8,9</sup>

The current challenge is the development of perovskite-based PV combining high PCE and operational stability. Published data on the stability and degradation mechanisms of perovskite-based PV are limited, although sensitivity of these materials to air/moisture and light exposure is evident.<sup>10–12</sup> While the efficiency can be measured within seconds, the time scale for stability assessment may be on the order of months or years, raising the need for relevant accelerated stability tests. The introduction of various stress conditions (heat, increased light intensity, oxygen/moisture environment, etc.) can

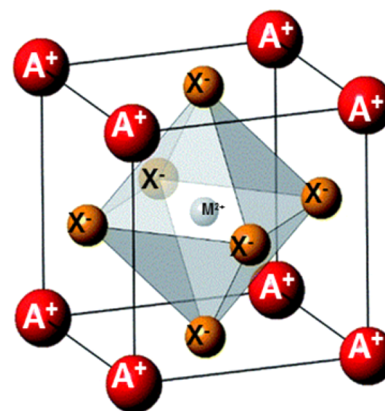


**Figure 1.** Organic–inorganic hybrid perovskite unit cell with [MX<sub>6</sub>]<sup>4–</sup> octahedral anion surrounded by organic cations in cubic arrangement. A, organic cation; M, divalent metal cation; X, halide anion.

accelerate the degradation rate relative to degradation under standard operational conditions. Recently we demonstrated the use of concentrated sunlight for organic PV-accelerated degradation testing.<sup>13–15</sup> Here we report the first results of accelerated degradation testing of MAPbX<sub>3</sub> films (X = I or Br)

**Received:** December 15, 2014

**Accepted:** December 30, 2014

**Published:** December 30, 2014

under exposure to concentrated sunlight of 100 suns (1 sun = 100 mW/cm<sup>2</sup>). One hour of such exposure provides a photon dose equivalent to that of one sun exposure for 100 hours. We show that the evolution of light absorption and corresponding structural modifications are dependent on the type of halide ion and the exposure temperature.

Figure 2 shows UV–vis absorption spectra of MAPbI<sub>3</sub> film exposed to 100 suns for various times ( $t = 0, 20, 40$ , and 60

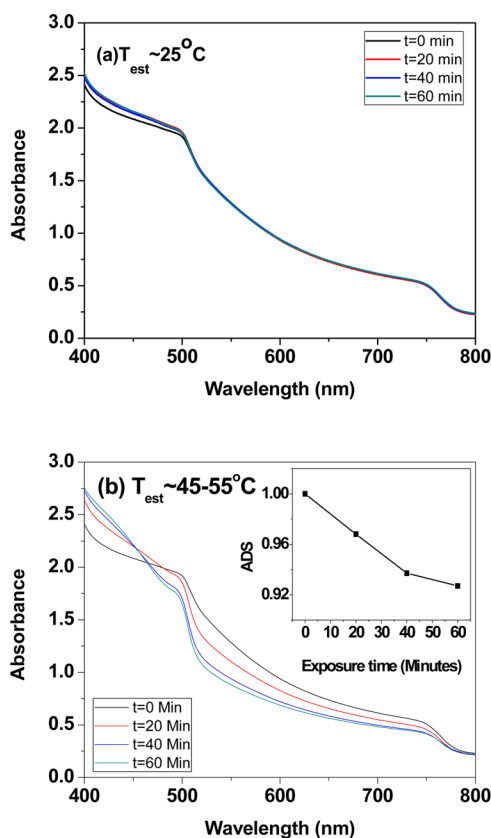


**Figure 2.** UV–vis absorption spectra of encapsulated MAPbI<sub>3</sub> films exposed to 100 suns for various times with the thermoelectric platform set to 5 (a) and 25 °C (b). The estimated temperatures of perovskite films  $T_{\text{est}}$  were  $\sim 25$  (a) and  $45\text{--}55$  °C (b). The inset in panel b shows the time evolution of the absorption degradation state (ADS), that is, the ratio of the number of absorbed solar photons for the exposed film to that for the as-produced film.

min) with the thermoelectric platform temperature set at 5 (a) and 25 °C (b). It should be noted that the temperature of the film on a glass substrate under concentrated sunlight is always higher than the set value of a thermoelectric platform. On the basis of our previous work,<sup>15</sup> we estimate the sample temperatures to be  $T_{\text{est}} \sim 25$  °C and  $45\text{--}55$  °C when the thermoelectric platform is set to 5 and 25 °C, respectively. The typical MAPbI<sub>3</sub> absorption spectrum shows strong absorption in the range of 400–520 nm and the onset at  $\sim 780$  nm corresponding to the material's optical band gap  $E_g = 1.58$  eV.<sup>7</sup> The absorption of a MAPbI<sub>3</sub> film after various exposure times to 100 suns, where  $T_{\text{est}}$  was  $\sim 25$  °C, was found to be unchanged (Figure 2a). On the contrary, the same sample exhibited a degradation in absorption after 100 suns exposure at  $T_{\text{est}} 45\text{--}55$  °C (Figure 2b). The original dark brown color of the film started fading in the illuminated area (just beneath the kaleidoscope) and finally became yellowish. We quantified the

degradation by calculating the ratio of the number of absorbed solar photons (from the AM1.5G spectrum) for the exposed film to that of the fresh sample as a function of the exposure time<sup>16</sup> (for the calculation method see Supporting Information). This ratio showed a slight gradual decrease with exposure time (by  $\sim 7\%$  for 60 min) (Figure 2b, inset).

Perusal of the data shown in Figure 2b can shed light on the photobleaching mechanism. Absorption in the range of 400–460 nm was found to increase with exposure time, and the formation of a hump between 400 and 480 nm became more prominent. Such absorption evolution suggests that decomposition of the hybrid perovskite material with crystallization of its inorganic component PbI<sub>2</sub> occurs during the exposure.<sup>10–12</sup> A possible pathway for such degradation under illumination in the presence of moisture was proposed by Niu et al.<sup>11</sup> It includes MAPbI<sub>3</sub> decomposition to PbI<sub>2</sub> and MAI with further dissociation of MAI to methyl amine, iodine, and water molecules. Frost et al.<sup>17</sup> suggested a slightly different decomposition mechanism in the presence of water, also resulting in the release of PbI<sub>2</sub>, MA, HI, and H<sub>2</sub>O. Either mechanism can explain our observations.

PbI<sub>2</sub> crystallization was directly confirmed by XRD measurements. Figure 3a,b shows XRD patterns of MAPbI<sub>3</sub> film in its

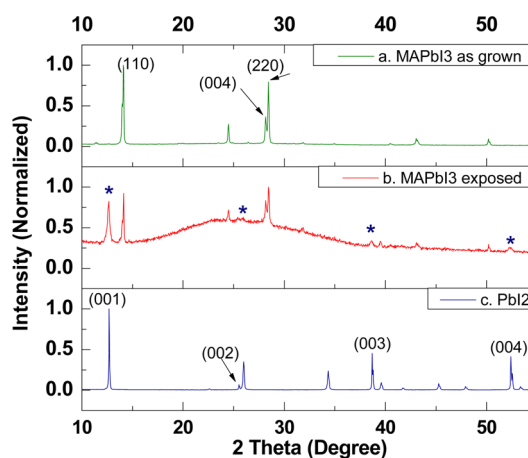


**Figure 3.** Normalized XRD patterns of (a,b) encapsulated MAPbI<sub>3</sub> film in as-produced state and after exposure to 100 suns at  $T_{\text{est}} \sim 45\text{--}55$  °C and (c) pristine PbI<sub>2</sub> powder. The peak intensities were normalized by the intensity of the highest peak in each case.

as-grown state and after 1 h of exposure to 100 suns at  $T_{\text{est}} \approx 45\text{--}55$  °C. The former diffractogram (Figure 3a) contains characteristic reflections of the MAPbI<sub>3</sub> perovskite tetragonal phase.<sup>18</sup> After exposure, the decreased intensities of these reflections and the appearance of the intensive reflection at  $12.6^\circ$  can be observed (Figure 3b). This peak is attributed to the (001) reflection of hexagonal PbI<sub>2</sub> (JCPDS-ICDD card 7–235). This and other peaks (marked with asterisks) in the exposed film's diffractogram coincide with XRD reflections from pristine PbI<sub>2</sub> powder (Figure 3c). The increased background in the exposed film's diffractogram (Figure 3b) may be related to the amorphous organic component (MAI, methylammonium iodide) of the decomposed film. Low-intensity peaks of tetragonal MAPbI<sub>3</sub> were also present in the exposed film's pattern (Figure 3b), indicating the incomplete decomposition of MAPbI<sub>3</sub> during the exposure.

Our results indicate the strong effect of heating on MAPbI<sub>3</sub> photobleaching under concentrated sunlight. To verify that the

degradation was caused by the exposure to concentrated sunlight, we also measured the absorption after sample annealing at elevated temperatures in the dark. Figure 4

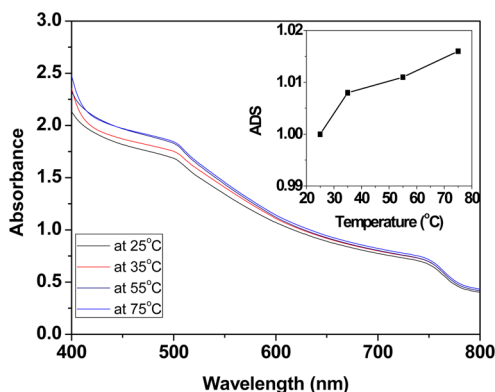


**Figure 4.** UV-vis absorption spectra of MAPbI<sub>3</sub> film before and after annealing for 1 h in the dark at 25, 35, 55, and 75 °C. The inset shows the temperature dependence of the absorption degradation state (ADS), that is, the ratio of the number of absorbed solar photons for the exposed film to that for the as-produced film.

shows the UV-vis absorption spectra of a MAPbI<sub>3</sub> film before and after annealing for 1 h in the dark at 25, 35, 55, and 75 °C. No photobleaching was observed. Furthermore, some increase in the absorption at the entire spectral range was evident. This may be attributed to improved crystallinity of the hybrid perovskite material after the annealing. These control experiments verify the role of illumination as an enhancing, possibly crucial, factor for the decomposition of MAPbI<sub>3</sub>. We therefore postulate that the decomposition mechanism of MAPbI<sub>3</sub> is light- and thermally enhanced or initiated.

The observed thermal enhancement of the photodegradation can be a manifestation of thermally accelerated chemical decomposition mechanisms previously discussed as well as a result of enhanced penetration of moisture/oxygen into the encapsulated samples due to thermally enhanced diffusion or due to degradation of the encapsulation. We note that the development of stable and efficient encapsulation is a necessary condition for industrialization of this novel photovoltaic technology.

Stability tests of the bromide counterpart MAPbBr<sub>3</sub> were compared with those of MAPbI<sub>3</sub>. Figure 5 shows the light absorption spectra of a MAPbBr<sub>3</sub> film exposed to 100 suns for various times at elevated sample temperature, that is,  $T_{\text{est}} \approx 45\text{--}55$  °C. No photobleaching was recorded. All spectra include the onset at  $\sim 540$  nm corresponding to the optical band gap of MAPbBr<sub>3</sub>,  $E_g \approx 2.3$  eV.<sup>19</sup> The MAPbBr<sub>3</sub> stability was supported by the lack of changes in the XRD patterns of these films before and after exposure (Figure S2 in the Supporting Information). A similar stability was observed for MAPbBr<sub>3</sub> films exposed at  $T_{\text{est}} \approx 25$  °C under similar conditions (Figure S3 in the Supporting Information). The demonstrated better stability of MAPbBr<sub>3</sub> films under concentrated sunlight is in agreement with such observations under 1-sun, which were obtained without encapsulation and under significantly smaller photon doses.<sup>10,20</sup>

The decomposition of MAPbI<sub>3</sub> was previously suggested to be induced by illumination in the presence of water and to be initiated by breaking one of the Pb–I bonds, followed by further decomposition steps.<sup>11,17</sup> We postulate that the better

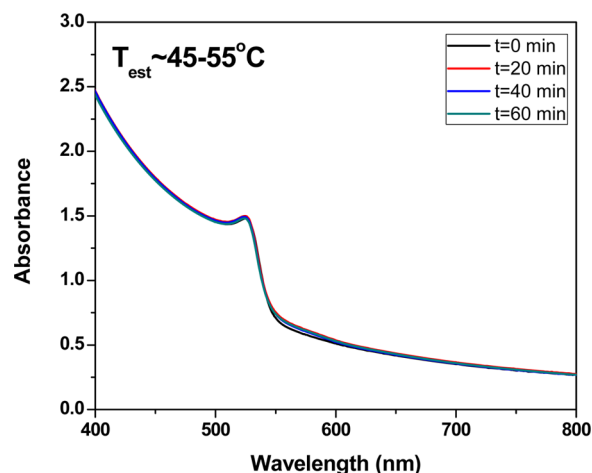


**Figure 5.** UV-vis absorption spectra of an encapsulated MAPbBr<sub>3</sub> film exposed to 100 suns for various times at  $T_{\text{est}} \approx 45\text{--}55$  °C.

stability of MAPbBr<sub>3</sub> perovskite films, compared with their iodide counterpart, results from differences in bond strengths and in their crystalline forms. The Pb–Br bond was calculated to be stronger and shorter compared with the Pb–I bond,<sup>21</sup> and hence its breaking is expected to be more difficult. In addition, hybrid halide perovskites are expected to be stabilized by halogen-(amine) hydrogen bonds.<sup>22,23</sup> The increased strength of the H–Br bond compared with the H–I bond, resulting from larger Br electronegativity, can further contribute to the relative stability of the MAPbBr<sub>3</sub> perovskite. Furthermore, at room temperature, the MAPbBr<sub>3</sub> crystal form is cubic with  $Pm\bar{3}m$  space group, whereas MAPbI<sub>3</sub> is in a distorted 3-D perovskite structure in tetragonal crystal arrangement with  $I4/mcm$  space group.<sup>24,25</sup> This structural difference between the two perovskite materials originates from the ionic radius difference between Br<sup>−</sup> and I<sup>−</sup> ions with six-fold symmetry, which are 1.96 and 2.2 Å, respectively.<sup>10,26</sup> Because cubic structures may be denser than tetragonal ones, they are expected to be less prone to attack by external species such as water. We note that despite the careful encapsulation used here, residual water may be present in the perovskite films and contribute to its decomposition.

Despite the better photochemical stability of MAPbBr<sub>3</sub> films, the higher optical band gap of this material ( $E_g \approx 2.3$  vs 1.58 eV for MAPbI<sub>3</sub>) would reduce the PV performance of MAPbBr<sub>3</sub> single junction devices.<sup>8</sup> We propose that MAPbBr<sub>3</sub> can be efficiently used as a top sub cell in future tandem architectures of perovskite-based PV. A mixed halide perovskite, MAPbI<sub>(3-x)</sub>Br<sub>x</sub>,<sup>10,16,18,27</sup> may also have the potential to achieve perovskite-based solar cells that combine high efficiency and stability.

In summary, the stability of encapsulated MAPbX<sub>3</sub> (X = I or Br) perovskite films was studied using concentrated sunlight. We have shown the photobleaching of MAPbI<sub>3</sub> films after exposure to 100 suns for 60 min at elevated sample temperatures ( $T_{\text{est}} \approx 45\text{--}55$  °C) due to decomposition of the hybrid perovskite material and crystallization of its inorganic component PbI<sub>2</sub>. No degradation was observed after MAPbI<sub>3</sub> film exposure to the same light intensity and dose but at lower sample temperatures ( $T_{\text{est}} \approx 25$  °C), indicating that degradation by photoinduced decomposition is thermally enhanced. Heat treatment of similar films in the dark did not result in degradation in the absorption or decomposition. We



therefore postulate that the observed degradation is induced/accelerated by a *combined* effect of light and heat during concentrated sunlight exposure and is possibly related to penetration of ambient species to the encapsulated samples.

MAPbBr<sub>3</sub> films demonstrated higher stability. No photo-bleaching or decomposition was observed after exposure of these films to similar stress conditions (light intensity, dose, and temperature). The better stability of MAPbBr<sub>3</sub> perovskite films, compared with their iodide counterpart, can possibly be related to differences in bond strengths and in crystalline forms between the two perovskites. A mixed halide perovskite, MAPbI<sub>(3-x)</sub>Br<sub>x</sub>, with a larger band gap than MAPbBr<sub>3</sub>, may therefore have the potential to achieve perovskite-based solar cells that combine high efficiency and stability.

Our results constitute a basis for further detailed investigations using longer exposure times and higher photon doses as well as comparing the effect of various light intensities with the same doses. Such further research should provide a deeper understanding of the mechanisms of degradation under various light intensities (including those for one sun) and a systematic comparison of the corresponding degradation rates. It can assist in the development of cross-validated accelerated stability testing of perovskite-based materials and solar cells with scaling relations between the degradation rates under photovoltaic operational conditions (one sun) and under concentrated sunlight.

## ■ EXPERIMENTAL METHODS

**Synthesis of Perovskites and Film Preparation.** MAPbI<sub>3</sub> and MAPbBr<sub>3</sub> films were deposited onto glass substrates using a procedure whose details were reported elsewhere<sup>20</sup> and encapsulated using a glass coverslip. In short, glass substrates were carefully cleaned and the perovskite films were deposited using the two-step synthesis method in a glovebox. In the first step, a concentrated solution of PbI<sub>2</sub> or PbBr<sub>2</sub> in DMF was spin-casted on the glass substrate, followed by annealing for 30 min at 90 °C. In the second step, the PbI<sub>2</sub>/PbBr<sub>2</sub> films were immersed in a 10 mg/mL solution of methylammoniumiodide (MAI)/methylammonium bromide (MABr), respectively, in isopropanol for 30 s, resulting in MAPbI<sub>3</sub>/MAPbBr<sub>3</sub> films, respectively. As-prepared perovskite films were annealed at 90 °C for another 30 min. The encapsulation of these films was done inside the glovebox using a DuPont Surlyn film as a spacer and sticker for the upper glass by melting it using a welding pen.

**Exposure of Films to Concentrated Sunlight.** Sunlight collected and concentrated outdoors was focused into a transmissive optical fiber and delivered indoors onto the sample (Figure S1a in the Supporting Information).<sup>28,29</sup> Flux uniformity was achieved with a 2.5 cm long, 0.25 cm<sup>2</sup> square cross-section kaleidoscope placed between the distal fiber tip and the sample (Figure S1b in the Supporting Information).<sup>29</sup> Sunlight exposures were performed in Sede Boquer (Lat. 30.8°N, Lon. 34.8°E, Alt. 475 m) during clear-sky periods around noontime, where the solar spectrum was found to be very close to the standard AM1.5G solar spectrum at that time.<sup>30</sup> The spectrum of light delivered to the sample was also close to the AM1.5G.<sup>24</sup> The concentration of sunlight delivered to the sample was measured using a spectrally blind pyranometer (thermopile) of 5% accuracy. During the exposure, the samples were thermally bonded to the top of a thermoelectric temperature controller, which was set at 5 or 25 °C. The temperature at the “sample/thermoelectric table” interface was measured with a thermo-

couple (T type) connected to the sample using a silver paste; that is, it measured the real sample temperature rather than that set for the thermoelectric table. Silver paste is an excellent heat conductor with high reflectivity, which minimized light absorption by the thermocouple itself.

**Optical and Crystallographic Characterization.** The UV–vis absorption spectra of the films were recorded using a Cary 5000 UV–vis–NIR spectrophotometer (Agilent Technologies). For control experiments, samples were annealed in the dark at 35, 55, or 75 °C for 1 h. X-ray diffraction (XRD) data were collected with Panalytical Empyrean powder diffractometer equipped with position-sensitive X'Celerator detector using Cu K<sub>α</sub> radiation ( $\lambda = 1.5405 \text{ \AA}$ ) and operated at 40 kV and 30 mA.

## ■ ASSOCIATED CONTENT

### Supporting Information

Schematic representation of solar concentrator, pre- and post-exposure UV–vis absorption spectra, X-ray diffraction patterns of MAPbBr<sub>3</sub> perovskite films and the calculation method of the number of absorbed solar photons. This material is available free of charge via the Internet at <http://pubs.acs.org>.

## ■ AUTHOR INFORMATION

### Corresponding Author

\*E-mail: [keugene@bgu.ac.il](mailto:keugene@bgu.ac.il).

### Notes

The authors declare no competing financial interest.

## ■ ACKNOWLEDGMENTS

R.K.M., E.A.K., and I.V.-F. acknowledge the support of the European Commission's StableNextSol COST Action MP1307. R.K.M. also thanks Blaustein Center for Scientific Cooperation for providing a postdoctoral research fellowship. This research was funded in part by a grant from the Adelis Foundation. L.E. acknowledges the support from Israel Alternative Energy Foundation (I-SAEF) that financed this research, the Ministry of Industry, Trade and Labor, Office of the Chief Scientist, Kamin project No. 50303, and the Tashtiot project of the Office of the Chief Scientist.

## ■ REFERENCES

- (1) Kojima, A.; Teshima, K.; Shirai, Y.; Miyasaka, T. Organometal Halide Perovskites as Visible Light Sensitizers for Photovoltaic Cells. *J. Am. Chem. Soc.* **2009**, *131*, 6050–6051.
- (2) Park, N. G. Organometal Perovskite Light Absorbers toward A 20% Efficiency Low Cost Solid State Mesoscopic Cells. *J. Phys. Chem. Lett.* **2013**, *4*, 2423–2429.
- (3) Service, R. F. Perovskite Solar Cells Keep On Surging. *Science* **2014**, *344*, 458.
- (4) [http://www.nrel.gov/ncpv/images/efficiency\\_chart.jpg](http://www.nrel.gov/ncpv/images/efficiency_chart.jpg).
- (5) Green, M. A.; Baillie, A. H.; Snaith, H. J. The Emergence of Perovskite Solar Cells. *Nat. Photonics* **2014**, *8*, 506–514.
- (6) Gamliel, S.; Etgar, L. Organo-Metal Perovskite Based Solar Cells: Sensitized versus Planar Architecture. *RSC Adv.* **2014**, *4*, 29012–29021.
- (7) Xu, X.; Randorn, C.; Efsthathiou, P.; Irvine, J. T. S. A Red Metallic Oxide Photocatalyst. *Nat. Mater.* **2012**, *11*, 595–598.
- (8) Etgar, L.; Gao, P.; Xue, Z.; Peng, Q.; Chandiran, A. K.; Liu, B.; Nazeeruddin, M. K.; Gratzel, M. Mesoscopic CH<sub>3</sub>NH<sub>3</sub>PbI<sub>3</sub>/TiO<sub>2</sub> Heterojunction Solar Cells. *J. Am. Chem. Soc.* **2012**, *134*, 17396–17399.
- (9) Chen, Z.; Li, H.; Tang, Y.; Huang, X.; Ho, D.; Lee, C. S. Shape Controlled Synthesis of Organolead Halide Perovskite Nanocrystals

and Their Tunable Optical Absorption. *Mater. Res. Express* **2014**, *1*, 015034-1–015034-10.

(10) Noh, J. H.; Im, S. H.; Heo, J. H.; Mandal, T. N.; Seok, S. I. Chemical Management for Colorful, Efficient, and Stable Inorganic–Organic Hybrid Nanostructured Solar Cells. *Nano Lett.* **2013**, *13*, 1764–1769.

(11) Niu, G.; Li, W.; Meng, F.; Wang, L.; Dong, H.; Qiu, Y. Study on the Stability of  $\text{CH}_3\text{NH}_3\text{PbI}_3$  Films and The Effect of Post Modification by Aluminum Oxide in All Solid State Hybrid Solar Cells. *J. Mater. Chem. A* **2014**, *2*, 705–710.

(12) Leijtens, T.; Epron, G. E.; Pathak, S.; Abate, A.; Lee, M. M.; Snaith, H. Overcoming Ultraviolet Light Instability of Sensitized  $\text{TiO}_2$  with Meso Superstructured Organometal Tri-Halide Perovskite Solar Cells. *Nat. Commun.* **2013**, *4*, 2885.

(13) Tromholt, T.; Katz, E. A.; Hirsch, B.; Vossier, A.; Krebs, F. C. Effects of Concentrated Sunlight on Organic Photovoltaics. *Appl. Phys. Lett.* **2010**, *96*, 73501-1–73501-3.

(14) Manor, A.; Katz, E. A.; Tromholt, T.; Krebs, F. C. Electrical and Photo-Induced Degradation of  $\text{ZnO}$  Layers in Organic Photovoltaics. *Adv. Energy Mater.* **2011**, *1*, 836–843.

(15) Visoly-Fisher, I.; Mescheloff, A.; Gabay, M.; Bounioux, C.; Zeiri, L.; Sansotera, M.; Goryachev, A. E.; Braun, A.; Galagan, Y.; Katz, E. A. Concentrated Sunlight for Accelerated Stability Testing of Organic Photovoltaic Materials: Towards Decoupling Light Intensity and Temperature. *Sol. Energy Mater. Sol. C* **2014**, *134*, 99–107.

(16) Tromholt, T.; Manceau, M.; Helgesen, M.; Carle, J. E.; Krebs, F. C. Degradation of Semiconducting Polymers by Concentrated Sunlight. *Sol. Energy Mater. Sol. C* **2011**, *95*, 1308–1314.

(17) Frost, J. M.; Butler, K. T.; Brivio, F.; Hendon, C. H.; Schilfgaarde, M. V.; Walsh, A. Atomistic Origins of High-Performance in Hybrid Halide Perovskite Solar Cells. *Nano Lett.* **2014**, *14*, 2584–2590.

(18) Baiki, T.; Fang, Y.; Kadro, J. M.; Schreyer, M.; Wei, F.; Mhaisalkar, S. G.; Graetzel, M.; White, T. J. Synthesis and Crystal Chemistry of the Hybrid Perovskites  $(\text{CH}_3\text{NH}_3)\text{PbI}_3$  For Solid State Sensitized Solar Cell Applications. *J. Mater. Chem. A* **2013**, *1*, 5628–5641.

(19) Ha, S. T.; Liu, X.; Zhang, Q.; Giovanni, D.; Sum, T. C.; Xiong, Q. Synthesis of Organic–Inorganic Lead Halide Perovskites Nanoplatelets: Towards High Performance Perovskites Solar Cells and Optoelectronic Devices. *Adv. Optical Mater.* **2014**, *2*, 838-1–838-7.

(20) Aharon, S.; Cohen, B. E.; Etgar, L. Hybrid Lead Halide Iodide and Lead Halide Bromide in Efficient Hole Conductor Free Perovskite Solar Cell. *J. Phys. Chem. C* **2014**, *118*, 17160–17165.

(21) Benavides-Garcia, M.; Balasubramanian, K. Bond Energies, Ionization Potentials, and The Singlet-Triplet Energy Separations Of  $\text{SnCl}_2$ ,  $\text{SnBr}_2$ ,  $\text{SnI}_2$ ,  $\text{PbCl}_2$ ,  $\text{PbBr}_2$ ,  $\text{PbI}_2$ , and their Positive Ions. *J. Chem. Phys.* **1994**, *100*, 2821–2830.

(22) Egger, D. A.; Kronik, L. Role of Dispersive Interactions in Determining Structural Properties of Organic–Inorganic Halide Perovskites: Insights from First-Principles Calculations. *J. Phys. Chem. Lett.* **2014**, *5*, 2728–2733.

(23) Mosconi, E.; Amat, A.; Nazeeruddin, M. K.; Grätzel, M.; Angelis, F. D. First-Principles Modeling of Mixed Halide Organometal Perovskites for Photovoltaic Applications. *J. Phys. Chem. C* **2013**, *117*, 13902–13913.

(24) Yamamuro, M. O.; Matsuo, T.; Hiroshi, S. Calorimetric and IR Spectroscopic Studies of Phase Transitions in Methylammonium-trihalogenplumbates (II). *J. Phys. Chem. Solids* **1990**, *51*, 1383–1395.

(25) Poglitsch, A.; Weber, D. Dynamic Disorder in Methylammonium-trihalogenplumbates (II) Observed by Millimeter wave Spectroscopy. *J. Chem. Phys.* **1987**, *87*, 6373–6378.

(26) Cheng, Z.; Lin, J. Layered Organic–Inorganic Hybrid Perovskites: Structure Optical Properties, Film Preparation Patterning and Templating Engineering. *J. Cryst. Eng. Comm.* **2010**, *12*, 2646–2662.

(27) Eperon, G. E.; Stranks, S. D.; Menelaou, C.; Johnston, M. B.; Herz, L. M.; Snaith, H. J. Formamidinium Lead Trihalide: A Broadly Tunable Perovskite for Efficient Planar Heterojunction Solar Cells. *Energy Environ. Sci.* **2014**, *7*, 982–988.

(28) Gordon, J. M.; Katz, E. A.; Feuermann, D.; Huleihil, M. Toward Ultra-High-Flux Photovoltaic Concentration. *Appl. Phys. Lett.* **2004**, *84*, 3642–3644.

(29) Katz, E. A.; Gordon, J. M.; Tasew, W.; Feuermann, D. Photovoltaic Characterization of Concentrator Solar Cells by Localized Irradiation. *J. Appl. Phys.* **2006**, *100*, 044514-1–044515-8.

(30) Berman, D.; Faiman, D. EVA Browning and the Time-Dependence of I–V Curve Parameters on PV Modules with and Without Mirror-Enhancement in a Desert Environment. *Sol. Energy Mater. Sol. Cells* **1997**, *45*, 401–412.